J. Fluid Mech. (1983), *vol.* 137, *pp.* 131–151
Printed in Great Britain

Generalized energy methods in electrohydrodynamic stability theory

By B. J. S. DEO† AND A. T. RICHARDSON
Department of Engineering Mathematics, University of Bristol, U.K.

(Received 6 August 1982 and in revised form 2 August 1983)

A generalized energy stability analysis necessarily incorporating charge-diffusion effects is applied to an electrohydrodynamic equilibrium comprising a dielectric liquid confined between two planar electrodes and subjected to an injection of unipolar charge. Generalized energy, kinetic-charge and mixed-type functionals are considered. Using the physical constraint that the sign of space-charge density can never change, it is possible to bound the nonlinear terms in the functional evolution equations. Sufficient conditions to guarantee global monotonic stability in the mean are then derived. In the case of a strong injection of charge the mixed-type functional provides theoretical values of the stability parameter close to the experimental values. Sufficient conditional stability bounds are also obtained for the leading-order diffusion-free equilibrium.

1. Introduction

In the last decade considerable experimental and theoretical effort has been directed towards explaining the effects of a d.c. electric field on a plane layer of dielectric liquid. In particular, the onset of fluid motion and the consequent augmentation of charge transfer has provided the impetus for a series of carefully controlled transient and steady-state electrochemical experiments and the application of appropriate mathematical instability analyses. By using ion-exchange membranes and electrodialytic varnishes on plane-parallel electrodes, it has been possible to investigate the consequences of almost space-charge-limited unipolar and bipolar injection into highly purified dielectric liquids and incorporate the modifying effects of residual conductivity. Atten & Lacroix (1978, 1979), considering the steady-state case of unipolar injection, established the existence of a hysteretical behaviour and found that the instability appeared in the form of a regular pattern of hexagonal cells. Two distinct values therefore were found for the critical stability parameter $T = \epsilon\Phi_0/\rho\nu K$, where Φ_0, ϵ, ρ, ν and K denote the applied d.c. potential, liquid permittivity, density and kinematic viscosity and the ion carrier mobility respectively. The higher value T_{lin} gave the applied voltage for which the hydrostatic steady electrodynamic equilibrium became unstable to small amplitude perturbations. On the other hand the lower value T_{fin} gave the voltage below which all finite-amplitude disturbances died out and the hydrostatic equilibrium state was recovered. Obviously, owing to inherent imperfections as well as difficulties in measuring system properties, the experiments provided a range of values so that $T_{\text{fin}} \approx 90 \pm 10$ and $T_{\text{lin}} \approx 100 \pm 10$ (Lacroix, Atten & Hopfinger 1975; Atten & Lacroix 1978, 1979).

The theoretical analyses most relevant to these latter steady-state unipolar-injection experiments in which both injecting and collecting surfaces were rigid were initiated by Atten & Moreau (1972). On making the simplifying assumptions that the liquid

† Present address: Gearhart Geodata Services Ltd., Aberdeen, Scotland.

was a perfect insulator, that injection was autonomous and that charge-diffusion effects were negligible, they obtained by a linear instability analysis a value for $T_{\text{lin}} \approx 160.750$ in the space-charge-limited currents limit. This limit corresponds to an infinite value of the space-charge parameter $C = Q_0 d^2/\epsilon \Phi_0$, where Q_0 is the charge density on the emitting surface and d is the gap between the electrodes. On retaining charge-diffusion effects in his linear instability analysis, Atten (1975, 1976) subsequently obtained crude estimates for $T_{\text{lin}} \approx 145 \pm 3$, 124 ± 2 and 110 for pyralenes, nitrobenzene and the very highly polar propylene carbonate respectively. On the other hand a nonlinear analysis of convective rolls by Atten & Lacroix (1974), using a mean-field approximation, gave in the case of large but finite injection ($C = 10$) a value $T_{\text{fin}} \approx 118$. More recently, however, using a modal approximation and a hexagonal planform, Atten & Lacroix (1978, 1979) have estimated, for the case of space-charge-limited currents, that $T_{\text{fin}} \approx 110$. Now relaxing the condition of autonomous injection undoubtedly modifies both T_{lin} and T_{fin}, but Atten & Lacroix (1974) have suggested that the latter is less sensitive to variations in the mechanism of injection. Furthermore, because of the high degree of purity of the experimental liquids, the predictions of a diffusionless linear instability analysis that incorporates residual conductivity effects (Atten 1975) still do not appear to give a satisfactory explanation of the discrepancy between theory and experiment.

All of the theoretical estimates to date have arisen from instability analyses and have consistently exceeded the experimental values. Alternatively an application of a generalized energy stability method (cf. Joseph 1976) can provide definite criteria that are sufficient for global and conditional asymptotic stability in the mean of the basic hydrostatic electrodynamic equilibrium. The formulation of such a theory requires a careful choice of positive-definite energy-type functionals. It is then possible to construct a variational problem tht leads in general to nonlinear Euler–Lagrange equations which, together with appropriate boundary conditions, constitute a differential eigenvalue problem whose eigenvalues correspond to critical values of the stability parameter T. These stability limits, because of the nonlinearities in the governing equations, are in general expected to be *conditional*, i.e. dependent upon the amplitude of the disturbance. However, in the present context, for certain choices of functional and by using a physical inequality constraint, it is possible to obtain linear Euler–Lagrange equations and consequently global stability limits. After obtaining the minimum eigenvalue τ and corresponding critical wavenumber α for a particular functional, it is then possible to maximize over any linking parameter λ so as to obtain the largest region of stability available within the theory.

2. Governing equations

Consider an incompressible dielectric liquid of constant density ρ, electrical permittivity ϵ and kinematic viscosity ν confined between two rigid planar perfectly conducting electrodes of infinite extent and distance d apart. Suppose that an autonomous injection of unipolar charge is emitted from the $z = 0$ electrode, which is maintained at potential Φ_0, and that the collecting electrode at $z = d$ is maintained at zero potential. The governing electrodynamic field equations in which magnetic effects have been neglected are

$$\boldsymbol{E} = -\nabla\Phi, \quad \nabla\cdot\boldsymbol{D} = Q, \quad \nabla\cdot\boldsymbol{J} = -\frac{\partial Q}{\partial t}, \tag{2.1}$$

where Φ, $\boldsymbol{E}$, $\boldsymbol{D}$, $\boldsymbol{J}$ and Q denote electrical potential, electric field, electric displacement,

current density and space-charge density respectively. Assuming further that the liquid is a linear isotropic dielectric and that charge is transported by convection, migration and diffusion, the additional electrical constitutive equations are

$$\boldsymbol{D} = \epsilon \boldsymbol{E}, \quad \boldsymbol{J} = Q\boldsymbol{U} + KQ\boldsymbol{E} - D_c \nabla Q, \tag{2.2}$$

where $\boldsymbol{U}$ is the liquid velocity and D_c is the charge-diffusion coefficient. To these must be added equations expressing the balance of linear momentum, in which the electrical force is Coulombic, and the conservation of mass. For a constant-density Newtonian fluid these reduce to

$$\frac{\partial \boldsymbol{U}}{\partial t} = -\boldsymbol{U}\cdot\nabla\boldsymbol{U} - \frac{1}{\rho}\nabla P + \nu\nabla^2\boldsymbol{U} + \frac{1}{\rho}Q\boldsymbol{E}, \quad \nabla\cdot\boldsymbol{U} = 0, \tag{2.3}$$

where P is the pressure.

Equations (2.1)–(2.3) may now be non-dimensionalized by making the following transformations:

$$\boldsymbol{x} \to d\boldsymbol{x}, \quad \Phi \to \Phi_0 \Phi, \quad \boldsymbol{E} \to \frac{\Phi_0}{d}\boldsymbol{E}, \quad Q \to \frac{\epsilon\Phi_0}{d^2}Q, \tag{2.4}$$

$$\boldsymbol{U} \to \frac{K\Phi_0}{d}\boldsymbol{U}, \quad t \to \frac{d^2}{\nu}t, \quad P \to \frac{\rho\nu K\Phi_0}{d^2}P,$$

so that velocity is scaled with respect to the ionic drift velocity and time with respect to the viscous decay time. Then without loss of generality Φ, $\boldsymbol{E}$ and Q are all non-negative. A dimensional analysis suggests that four non-dimensional parameters are required for a full specification of the problem. We need to quantify the applied potential, the electrical current, the ionic carrier mobility and characterize the particular dielectric liquid under consideration. For convenience we choose the following non-dimensional groupings:

$$T = \frac{\epsilon\Phi_0}{\rho\nu K}, \quad C = \frac{Q_0 d^2}{\epsilon\Phi_0}, \quad M = \frac{1}{K}\left(\frac{\epsilon}{\rho}\right)^{\frac{1}{2}}, \quad S = \frac{\epsilon D_c}{\rho\nu K^2}, \tag{2.5}$$

where the parameter T represents the ratio of the Coulombic forces to viscous forces, C is a measure of the injected charge, M is the ratio of hydrodynamic mobility to ionic mobility, and S is a new parameter, taking values for typical experimental dielectric liquids in the range 0.04–0.4, which enters because we have retained charge-diffusion effects. Equations (2.1)–(2.3) then reduce to

$$\begin{aligned}
\frac{\partial \boldsymbol{U}}{\partial t} &= -\frac{T}{M^2}\boldsymbol{U}\cdot\nabla\boldsymbol{U} - \nabla P + \nabla^2\boldsymbol{U} + TQ\boldsymbol{E}, \\
\frac{\partial Q}{\partial t} &= -\frac{T}{M^2}\boldsymbol{U}\cdot\nabla Q - \frac{T}{M^2}\nabla\cdot(Q\boldsymbol{E}) + \frac{S}{M^2}\nabla^2 Q, \\
\boldsymbol{E} &= -\nabla\Phi, \quad \nabla\cdot\boldsymbol{E} = Q, \quad \nabla\cdot\boldsymbol{U} = 0.
\end{aligned} \tag{2.6}$$

It is worth noting that the grouping $T/M^2 = K\Phi_0/\nu$ is a Reynolds number based on the ionic velocity and that $S/M^2 = D_c/\nu$ is an inverse electric Prandtl number.

Generalized energy methods applied to infinite domains require the construction of spatially averaged integrals. We could choose to average over a 'periodic cell' of

length X_0 in the x-direction, Y_0 in the y-direction, and of volume $\mathscr{V}_0$. We could then define the volume average of a scalar field ψ by

$$\langle\psi\rangle \equiv \frac{1}{\mathscr{V}_0}\int_0^{X_0}\int_0^{Y_0}\int_0^1 \psi(x,y,z,t)\,\mathrm{d}x\,\mathrm{d}y\,\mathrm{d}z, \tag{2.7}$$

and a volume-averaged surface integral of a vector field $\boldsymbol{f}$ by

$$\langle \boldsymbol{f}\rangle_{\mathscr{S}} \equiv \frac{1}{\mathscr{V}_0}\int_{\mathscr{S}_0} \boldsymbol{f}\cdot\mathbf{d}\mathscr{S}, \tag{2.8}$$

where $\mathbf{d}\mathscr{S}$ is a vector element of the surface $\mathscr{S}_0$ enclosing the volume $\mathscr{V}_0$. However, by averaging over the entire layer, we can extend these definitions to include almost-periodic functions (cf. Joseph 1976) in the subsequent analysis. Then, allowing $\boldsymbol{U}$ to be an almost-periodic solenoidal vector field vanishing on the rigid boundaries $z = 0$ and $z = 1$, the Reynolds transport theorem permits us to express the Lagrangian time derivative of the volume average of a scalar field ψ as

$$\frac{\mathrm{d}}{\mathrm{d}t}\langle\psi\rangle = \left\langle\frac{\partial\psi}{\partial t}\right\rangle. \tag{2.9}$$

From (2.6) we can therefore deduce that

$$\frac{\mathrm{d}}{\mathrm{d}t}\langle\tfrac{1}{2}|\boldsymbol{U}|^2\rangle = T\langle Q\boldsymbol{E}\cdot\boldsymbol{U}\rangle - \langle|\boldsymbol{\nabla U}|^2\rangle, \tag{2.10}$$

$$\frac{\mathrm{d}}{\mathrm{d}t}\langle\tfrac{1}{2}Q^2\rangle = -\frac{T}{2M^2}\langle Q^3\rangle - \frac{S}{M^2}\langle|\boldsymbol{\nabla}Q|^2\rangle - \frac{T}{2M^2}\langle Q^2\boldsymbol{E}\rangle_{\mathscr{S}} + \frac{S}{M^2}\langle Q\boldsymbol{\nabla}Q\rangle_{\mathscr{S}}, \tag{2.11}$$

from which it can be seen that $T\langle Q\boldsymbol{E}\cdot\boldsymbol{U}\rangle$ is an energy-production integral which couples the charge and electric-field distributions to the kinetic energy of the liquid motion. Moreover, since the scaled total charge $Q \geqslant 0$, we see that charge can only be increased by surface effects, as might have been expected from the physical simplifications implied in the model.

Now the governing equations (2.6) possess a steady one-dimensional hydrostatic equilibrium solution in which electrical potential $\Phi_{\mathrm{e}}(z)$ satisfies the nonlinear equation

$$\frac{S}{T}\frac{\mathrm{d}^4\Phi_{\mathrm{e}}}{\mathrm{d}z^4} + \frac{1}{2}\frac{\mathrm{d}^2}{\mathrm{d}z^2}\left(\frac{\mathrm{d}\Phi_{\mathrm{e}}}{\mathrm{d}z}\right)^2 = 0 \tag{2.12}$$

and is subject to boundary conditions

$$\Phi_{\mathrm{e}}(0) = 1, \quad \Phi_{\mathrm{e}}(1) = 0, \quad \frac{\mathrm{d}^2}{\mathrm{d}z^2}\Phi_{\mathrm{e}}(0) = -C, \quad \frac{\mathrm{d}^2\Phi(1)}{\mathrm{d}z^2} = 0. \tag{2.13}$$

The first two conditions follow from the fixing of potential on each of the electrodes. The latter two constitute an injection and an ejection law specifying how charge is introduced and removed from the liquid layer. There exists an exact solution of (2.12) in terms of Airy functions, but specific evaluation of the equilibrium requires numerical analysis (cf. Deo & Richardson 1983). In most dielectric-fluid experiments the parameter $S/T = D_{\mathrm{c}}/K\Phi_0$ is small, and so the solution $\Phi_{\mathrm{e}}(z)$ exhibits a mainstream and boundary-layer character (cf. Richardson 1980). To leading order this mainstream solution for which $\boldsymbol{E} = E_{\mathrm{e}}(z)\,\boldsymbol{i}_z$ with corresponding space-charge density $Q = Q_{\mathrm{e}}(z)$ can be specified by

$$E_{\mathrm{e}}(z) = +\left(\frac{J^2}{C^2} + 2Jz\right)^{\frac{1}{2}}, \quad Q_{\mathrm{e}}(z) = \frac{J}{E_{\mathrm{e}}(z)}, \tag{2.14}$$

where J is a real constant uniquely determined by the cubical boundary constraint

$$J^3+(2C-1)CJ^2+\frac{4C^4J}{3}-\frac{3C^4}{2}=0. \tag{2.15}$$

The time evolution of nonlinear perturbations $\boldsymbol{u}$, $\boldsymbol{e}$ and q in liquid velocity, electric field and space-charge density of the equilibrium given by (2.14) and (2.15) is governed by equations

$$\frac{\partial \boldsymbol{u}}{\partial t}=-\frac{T}{M^2}\boldsymbol{u}\cdot\boldsymbol{\nabla}\boldsymbol{u}-\boldsymbol{\nabla}p+\nabla^2\boldsymbol{u}+T[q\boldsymbol{E}+Q\boldsymbol{e}+q\boldsymbol{e}], \tag{2.16a}$$

$$\frac{\partial \boldsymbol{e}}{\partial t}=\boldsymbol{b}-\frac{T}{M^2}[Q\boldsymbol{u}+q\boldsymbol{u}+q\boldsymbol{E}+Q\boldsymbol{e}+q\boldsymbol{e}]+\frac{S}{M^2}\boldsymbol{\nabla}q, \tag{2.16b}$$

$$\frac{\partial q}{\partial t}=-\frac{T}{M^2}[\boldsymbol{u}\cdot\boldsymbol{\nabla}Q+\boldsymbol{u}\cdot\boldsymbol{\nabla}q]-\frac{T}{M^2}\boldsymbol{\nabla}\cdot[q\boldsymbol{E}+Q\boldsymbol{e}+q\boldsymbol{e}]+\frac{S}{M^2}\nabla^2q, \tag{2.16c}$$

$$\boldsymbol{e}=-\boldsymbol{\nabla}\phi, \quad \boldsymbol{\nabla}\cdot\boldsymbol{e}=q, \quad \boldsymbol{\nabla}\cdot\boldsymbol{u}=0, \tag{2.16d,e,f}$$

where (2.16b) has been derived by integration of (2.16c), p is the perturbation in pressure and ϕ the perturbation in potential, $\boldsymbol{b}$ is an arbitrary solenoidal vector field, and the suffix e has been omitted. Since we are considering a unipolar injection of charge, we must in addition impose the physical constraint

$$Q+q\geqslant 0, \tag{2.17}$$

which corresponds to the fact that nowhere in the liquid can the charge density change sign. On forming the appropriate inner products and using the vanishing of both ϕ and $\boldsymbol{u}$ on the electrodes, we can readily deduce from (2.16) the time-evolution integral equations

$$\frac{\mathrm{d}}{\mathrm{d}t}\langle\tfrac{1}{2}|\boldsymbol{u}|^2\rangle=T\langle q\boldsymbol{E}\cdot\boldsymbol{u}+(Q+q)\,\boldsymbol{e}\cdot\boldsymbol{u}\rangle-\langle|\boldsymbol{\nabla}\boldsymbol{u}|^2\rangle, \tag{2.18}$$

$$\frac{\mathrm{d}}{\mathrm{d}t}\langle\tfrac{1}{2}|\boldsymbol{e}|^2\rangle=-\frac{T}{M^2}\langle q\boldsymbol{E}\cdot\boldsymbol{e}+(Q+q)\,(|\boldsymbol{e}|^2+\boldsymbol{e}\cdot\boldsymbol{u})\rangle-\frac{S}{M^2}\langle q^2\rangle+\frac{S}{M^2}\langle q\boldsymbol{e}\rangle_{\mathscr{S}}, \tag{2.19}$$

$$\frac{\mathrm{d}}{\mathrm{d}t}\langle\tfrac{1}{2}q^2\rangle=-\frac{T}{M^2}\langle q\boldsymbol{u}\cdot\boldsymbol{\nabla}Q+q\boldsymbol{\nabla}\cdot(q\boldsymbol{E}+Q\boldsymbol{e}+q\boldsymbol{e})\rangle-\frac{S}{M^2}\langle|\boldsymbol{\nabla}q|^2\rangle+\frac{S}{M^2}\langle q\boldsymbol{\nabla}q\rangle_{\mathscr{S}}. \tag{2.20}$$

The time rate of change of any positive-definite generalized energy functional comprising a linear combination of $|\boldsymbol{u}|^2$, $|\boldsymbol{e}|^2$ and q^2 will consequently not be homogeneous of degree two in the disturbances. Indeed it will involve both quadratic and cubic nonlinearities. This implies that it would not be possible directly to obtain a criterion for monotonic stability which is independent of the amplitude of the disturbance. However, by using the physical constraint (2.17) we can bound these cubic terms to obtain a lower estimate of the stability criterion. By using suitable trial functions we can also obtain an upper estimate. At the same time of course we can bound the cubic terms in a different fashion and obtain conditional stability limits that depend upon the functional's initial ($t=0$) value. In the next sections we will consider three functionals:

(*a*) a weighted energy functional

$$\mathscr{E}_1(t;\lambda)=\tfrac{1}{2}\langle|\boldsymbol{u}|^2+\lambda M^2|\boldsymbol{e}|^2\rangle, \tag{2.21}$$

(*b*) a kinetic-charge functional

$$\mathscr{E}_2(t;\lambda) = \tfrac{1}{2}\langle |\boldsymbol{u}|^2 + \lambda M^2 q^2 \rangle, \tag{2.22}$$

(*c*) a mixed functional

$$\mathscr{E}_3(t;\lambda) = \tfrac{1}{2}\langle |\boldsymbol{u}|^2 + M^2|\boldsymbol{e}|^2 + \lambda M^2 q^2 \rangle, \tag{2.23}$$

where λ is a scalar linking parameter, having noted that the coupling integral average $\langle \boldsymbol{e}\cdot\boldsymbol{u} \rangle = 0$.

3. Generalized energy stability analysis

Having decided upon a suitable generalized energy functional $\mathscr{E}(t;\lambda)$ incorporating the linking parameter λ, we can form the evolution equation

$$\frac{\mathrm{d}\mathscr{E}}{\mathrm{d}t} = T\mathcal{J} + \mathcal{S} - \mathcal{D}, \tag{3.1}$$

where volume production integral $\mathcal{J}$, surface production integral $\mathcal{S}$ and positive-definite dissipation integral $\mathcal{D}$ are explicitly independent of the stability parameter T. Whilst $\mathcal{D}$ is quadratic in the perturbations, in the present context both $\mathcal{J}$ and $\mathcal{S}$ are in general cubic. If, for fixed values of the parameters C, M and S, we define $\tau = \tau(\lambda, T)$ and $\Lambda = \Lambda(\lambda)$ by

$$\tau^{-1} = \max_{\boldsymbol{H}} \left(\frac{\mathcal{J} + \mathcal{S}/T}{\mathcal{D}} \right), \quad \Lambda^{-1} = \max_{\boldsymbol{H}} \left(\frac{\mathscr{E}}{\mathcal{D}} \right), \tag{3.2), (3.3}$$

we can then write

$$\frac{\mathrm{d}\mathscr{E}}{\mathrm{d}t} \leqslant -T\Lambda \left(\frac{1}{T} - \frac{1}{\tau} \right) \mathscr{E}. \tag{3.4}$$

Here $\boldsymbol{H}(\phi, \boldsymbol{u})$ is the space of kinematically admissible almost-periodic functions specified by

$$\boldsymbol{H} = \{(\phi, \boldsymbol{u}) : \nabla^2\phi \leqslant Q(z),\ \phi|_{z=0} = \phi|_{z=1} = 0;\ \nabla\cdot\boldsymbol{u} = 0,\ \boldsymbol{u}|_{z=0} = \boldsymbol{u}|_{z=1} = 0\}. \tag{3.5}$$

Since the basic equilibrium state is steady, integration of the inequality (3.4) leads to a bounding envelope of the functional so that

$$\mathscr{E}(t;\lambda) \leqslant \mathscr{E}(0;\lambda) \exp\left[-2\Lambda \left(\frac{1}{T} - \frac{1}{\tau} \right) t \right], \tag{3.6}$$

for $t \geqslant 0$. The critical value of the stability parameter $\bar{\tau}$, below which the functional $\mathscr{E}(t;\lambda)$ decays to zero monotonically with time and independently of its initial amplitude $\mathscr{E}(0;\lambda)$, is determined by the solution of the equation

$$\tau(\lambda, \bar{\tau}) = \bar{\tau}. \tag{3.7}$$

In this sense we have global monotonic stability of the basic state for $T < \bar{\tau}$. Although an individual component of the functional $\mathscr{E}(t;\lambda)$ could well increase initially, it must ultimately decay. Since our choice of linking parameter λ is arbitrary we can further seek an optimized value $\bar{\bar{\tau}}$ of $\bar{\tau}$ defined by

$$\bar{\bar{\tau}}^{-1} = \min_{\lambda} \bar{\tau}^{-1}. \tag{3.8}$$

The corresponding decay rate measure Λ can then be evaluated at $\bar{\bar{\lambda}}$, the optimizing value of positive real-valued λ.

Since the maximum problem (3.2) leads to nonlinear Euler–Lagrange equations,

we can avoid analytical complexity by using the physical constraint (2.17) to bound the cubic functionals $\mathcal{J}$ and $\mathcal{S}$ by quadratic functionals $\mathcal{J}_q$ and $\mathcal{S}_q$ and hence define

$$\tau_1^{-1} = \max_H\left(\frac{\mathcal{J}_q+\mathcal{S}_q/T}{\mathcal{D}}\right) \geqslant \max_H\left(\frac{\mathcal{J}+\mathcal{S}/T}{\mathcal{D}}\right) = \tau^{-1}. \tag{3.9}$$

Alternatively, by retaining the cubic functionals we can, by use of suitable trial functions, obtain a suboptimal value τ_2^{-1} of τ^{-1}. Consequently we have both upper and lower bounds for the exact value τ so that

$$\tau_1 \leqslant \tau \leqslant \tau_2. \tag{3.10}$$

From this it follows that $\bar{\tau}_1 \leqslant \bar{\tau} \leqslant \bar{\tau}_2$ and that $\bar{\bar{\tau}}_1(\bar{\bar{\lambda}}) \leqslant \bar{\bar{\tau}}(\bar{\bar{\lambda}}) \leqslant \bar{\bar{\tau}}_2(\bar{\bar{\lambda}})$.

If, on the other hand, we define

$$\tau_\ell^{-1} = \max_H\left(\frac{\mathcal{J}_0+\mathcal{S}_0/T}{\mathcal{D}}\right), \quad \Lambda^{-1} = \max_H\left(\frac{\mathscr{E}}{\mathcal{D}}\right), \tag{3.11), (3.12}$$

where $\mathcal{J}_0$ and $\mathcal{S}_0$ are the quadratic parts of the cubic functionals $\mathcal{J}$ and $\mathcal{S}$, we can obtain an inequality

$$\frac{\mathrm{d}\mathscr{E}}{\mathrm{d}t} \leqslant -T\left[\left(\frac{1}{T}-\frac{1}{\tau_\ell}\right)-G\mathscr{E}^{\frac{1}{2}}\right]\mathcal{D}, \tag{3.13}$$

where $G(\lambda)$ is a positive constant that arises from analytically bounding the cubic parts of $\mathcal{J}$ and $\mathcal{S}$ in terms of $\mathscr{E}$ and $\mathcal{D}$. Then for all initial amplitudes

$$\mathscr{E}(0;\lambda) \leqslant \left(\frac{1}{T}-\frac{1}{\tau_\ell}\right)^2\frac{1}{G^2} \tag{3.14}$$

it follows that

$$\frac{\mathscr{E}(t;\lambda)}{\left[\left(\frac{1}{T}-\frac{1}{\tau_\ell}\right)-G\mathscr{E}^{\frac{1}{2}}(t;\lambda)\right]^2} \leqslant \frac{\mathscr{E}(0;\lambda)}{\left[\left(\frac{1}{T}-\frac{1}{\tau_\ell}\right)-G\mathscr{E}^{\frac{1}{2}}(0;\lambda)\right]^2}\exp\left[-\left(1-\frac{T}{\tau_\ell}\right)\Lambda t\right]. \tag{3.15}$$

Hence $\bar{\tau}_\ell = \tau_\ell(\lambda, \bar{\tau}_\ell)$ is a zero-amplitude conditional stability limit. As before, we can optimize over λ and define $\bar{\bar{\tau}}_\ell$. Equation (3.14) then prescribes an approximate attracting radius for conditionally stable disturbances of the equilibrium state.

In the subsequent analysis we find that with the appropriate boundary conditions from the Euler–Lagrangian theory we have $\mathcal{S} \equiv 0$. If we consider the diffusion-free mainstream approximation (2.14) and (2.15) and accordingly neglect the ejection law corresponding to the fourth condition (2.13), the functional $\mathcal{J}$ is totally independent of T. Then $\bar{\tau} \equiv \tau$. Whilst at first sight a stability analysis incorporating diffusion effects of a diffusion-free equilibrium may appear somewhat inconsistent, the results of such an approximation to the full diffusion analysis are presented for comparison. Furthermore, the existence of finite-valued τ_1^{-1}, τ_ℓ^{-1} and Λ^{-1} is guaranteed by proofs similar to that given for τ_ℓ in the Appendix. Their respective values are therefore obtained by determining the lowest eigenvalue of a linear Euler–Lagrangian differential system.

4. The weighted energy functional

If we consider the functional defined by (2.21), we find, on using (2.18) and (2.19), that its time evolution is governed by

$$\frac{\mathrm{d}\mathscr{E}_1}{\mathrm{d}t} = T\langle q\boldsymbol{E}\cdot(\boldsymbol{u}-\lambda\boldsymbol{e})-(Q+q)\left[\lambda|\boldsymbol{e}|^2+(\lambda-1)\,\boldsymbol{e}\cdot\boldsymbol{u}\right]\rangle+\lambda S\langle q\boldsymbol{e}\rangle_{\mathscr{S}}-\langle|\boldsymbol{\nabla u}|^2+\lambda Sq^2\rangle, \tag{4.1}$$

so that $\mathcal{J}$ is cubic and both $\mathcal{S}$ and $\mathcal{D}$ are quadratic in the perturbations (cf. (3.1)).

4.1. *A global monotonic bound*

In the special case $\lambda = 1$ this functional is just the total energy of the perturbation, and the cubic term $\langle q\boldsymbol{e}\cdot\boldsymbol{u}\rangle$ does not appear. Furthermore, the cubic term $\langle q|\boldsymbol{e}|^2\rangle$ using inequality (2.17) can be avoided so that only quadratic functionals remain. The lower bound τ_1 is then defined by

$$\tau_1^{-1} = \max_{H}\left(\frac{\langle q\boldsymbol{E}\cdot(\boldsymbol{u}-\boldsymbol{e})\rangle + (S/T)\langle q\boldsymbol{e}\rangle_{\mathscr{S}}}{\langle|\nabla\boldsymbol{u}|^2 + Sq^2\rangle}\right) \tag{4.2}$$

and Λ by

$$\Lambda^{-1} = \max_{H}\left(\frac{\langle|\boldsymbol{u}|^2 + M^2|\boldsymbol{e}|^2\rangle}{2\langle|\nabla\boldsymbol{u}|^2 + Sq^2\rangle}\right). \tag{4.3}$$

The importance of a non-zero value for S in this analysis is readily apparent. If $S = 0$ then finite maxima do not exist and $\tau_1 = \Lambda = 0$. Diffusion effects therefore are paramount in such a stability analysis.

The linear Euler–Lagrange equations associated with the maximum problem (4.2) are

$$\frac{2}{\tau_1}\nabla^2(\nabla\wedge\boldsymbol{u}) + \nabla q\wedge\boldsymbol{E} = 0, \tag{4.4}$$

$$\nabla^2\left[\frac{2Sq}{\tau_1} + \boldsymbol{E}\cdot(\boldsymbol{e}-\boldsymbol{u})\right] - \nabla\cdot(q\boldsymbol{E}) = 0, \tag{4.5}$$

where we have used the fundamental lemmas for scalar and solenoidal vector fields of the variational calculus. In addition we find that the variational method leaves us with a surface integral

$$\langle(|\boldsymbol{e}|^2 + \boldsymbol{E}\cdot\boldsymbol{e})\,\boldsymbol{e}' + \frac{S}{\tau_1}(q\boldsymbol{e}' - q'\boldsymbol{e})\rangle_{\mathscr{S}} = 0, \tag{4.6}$$

where $'$ indicates an arbitrary variation. Equations (4.4) and (4.5) together with (2.16*d–f*) constitute an eighth-order differential system. Accordingly we must impose eight boundary conditions. Six of these are essential, i.e. those of no slip and fixed potential, and the remaining two are to be obtained from condition (4.6). If we choose these to be the essential conditions $\boldsymbol{e} = 0$ on $z = 0$ and $z = 1$ then (4.6) is certainly satisfied. We now restrict our class of kinematically admissible functions to $\boldsymbol{H}^*$, where

$$\boldsymbol{H}^* = \boldsymbol{H}(\phi, u)\cap\{\phi : \nabla\phi|_{z=0} = \nabla\phi|_{z=1} = 0\}. \tag{4.7}$$

This means as previously mentioned that the surface integral in (4.1) vanishes.

On Fourier-decomposing $\boldsymbol{u} = [u, v, w]$ and ϕ into normal modes so that

$$\begin{aligned}(u, v) &= [U(z), V(z)]\cos(kx+ly),\\ (w, \phi) &= [W(z), \Phi(z)]\sin(kx+ly),\end{aligned} \tag{4.8}$$

and on writing $\alpha^2 = k^2 + l^2$ and $\mathrm{D} = \mathrm{d}/\mathrm{d}z$, we find that the variational problem (4.2) is equivalent to the eighth-order differential eigenvalue problem

$$\frac{2}{\tau_1}(\mathrm{D}^2-\alpha^2)^2 W + \alpha^2 E(\mathrm{D}^2-\alpha^2)\Phi = 0, \tag{4.9}$$

$$\frac{2S}{\tau_1}(\mathrm{D}^2-\alpha^2)^2\Phi + [(\mathrm{D}E)\,\mathrm{D}^2 + (\mathrm{D}^2E)\,\mathrm{D} + \alpha^2(\mathrm{D}E)]\Phi + (\mathrm{D}^2-\alpha^2)(EW) = 0, \tag{4.10}$$

subject to boundary conditions

$$W = \mathrm{D}W = \Phi = \mathrm{D}\Phi = 0 \quad (z = 0, 1). \tag{4.11}$$

C	α_{crit}	$\bar{\tau}_1$	$\bar{\tau}_2$
(0)	(5.643)	(5.83192)	(5.91) [$a = 5.5$]
0.001	5.644	5.8327	5.91
	(5.643)	(5.83265)	(5.91) [$a = 5.5$]
0.01	5.641	5.8392	5.95
	(5.639)	(5.83917)	(5.95) [$a = 5.5$]
0.1	5.608	5.8986	6.30
	(5.607)	(5.89855)	(6.31) [$a = 5.5$]
1	5.378	6.1241	8.64 [$a = 6.5$]
	(5.381)	(6.11887)	(8.83) [$a = 5.5$]
10	0	4.5212	10.90
	(5.113)	(5.99969)	(10.33) [$a = 7.5$]
100	0	2.4193	11.13 [$a = 8.0$]
	(5.101)	(5.98673)	(10.37) [$a = 7.5$]
1000	0	0.92898	11.03 [$a = 8.0$]
	(5.100)	(5.98657)	(10.37) [$a = 7.5$]
(∞)	(5.100)	(5.98657)	(10.37) [$a = 7.5$]

TABLE 1. Numerical values of the global monotonic stability bound $\bar{\tau}_1$ and corresponding critical wavenumber α_{crit} together with trial-function estimates $\bar{\tau}_2$ at specified x-wavenumber a for the energy functional $\mathscr{E}_1(t;1)$ in the case $S = 0.1$. Results in parentheses are those obtained for the diffusion-free equilibrium.

The values of $\bar{\tau}_1$ minimized over wavenumber α for various values of C for both the diffusion and diffusion-free equilibrium in the special case $S = 0.1$ were obtained numerically, and together with estimates $\bar{\tau}_2$, using y-independent trial functions of the form

$$\phi = (1-\cos 2\pi z)\sin ax, \tag{4.12}$$

$$\boldsymbol{u} = \left[\sin 2\pi z \cos ax,\ 0,\ \frac{a}{2\pi}(1-\cos 2\pi z)\sin ax\right], \tag{4.13}$$

where a is an x-directional wavenumber, are presented in table 1.

Similarly the Euler–Lagrange equations for the variational problem (4.3) governing the decay rate

$$\frac{2S}{\Lambda M^2}\nabla^4\phi + \nabla^2\phi = 0, \quad \frac{2}{\Lambda}\nabla^2(\nabla\wedge\boldsymbol{u}) + \nabla\wedge\boldsymbol{u} = 0, \quad \nabla\cdot\boldsymbol{u} = 0, \tag{4.14}$$

on Fourier-decomposing, become

$$\left(\mathrm{D}^2-\alpha_\Phi^2+\frac{\Lambda M^2}{2S}\right)(\mathrm{D}^2-\alpha_\Phi^2)\,\Phi = 0, \quad (\mathrm{D}^2-\alpha_W^2+\tfrac{1}{2}\Lambda)(\mathrm{D}^2-\alpha_W^2)\,W = 0, \tag{4.15}$$

subject to the boundary conditions (4.11). Clearly, since there is electrical and fluid-dynamic decoupling, if the electrical Prandtl number $M^2/S = \nu/D_c \neq 1$, one and only one of Φ and W must vanish identically. Numerical integration indicates that

$$\Lambda \approx 74.162\min\left(\frac{S}{M^2}, 1\right), \quad \boldsymbol{\alpha}_{\text{crit}} = (\alpha_{\Phi\,\text{crit}}, \alpha_{W\,\text{crit}}) = (2.399, 2.399). \tag{4.16}$$

Hence if $M^2/S > 1$ we must choose $W \equiv 0$, whilst for $M^2/S < 1$ we must choose $\Phi \equiv 0$. This is perhaps to be expected, since in the former (latter) case viscous

C	$\bar{\bar{\lambda}}$	α_{crit}	$\bar{\bar{\tau}}_\ell$
0	—	3.95	—
0.001	2.78×10^7	3.95	8.0194×10^4
0.01	2.80×10^5	3.95	8.0555×10^3
0.1	3.07×10^3	3.95	841.978
1	69.0	3.995	124.375
10	22.3	4.134	68.001
100	21.65	4.143	68.803
1000	21.64	4.143	66.791
∞	21.64	4.143	66.791

TABLE 2. Numerical values of the conditional stability bound $\bar{\bar{\tau}}_\ell$ with corresponding critical wavenumber α_{crit} and optimal linking parameter $\bar{\bar{\lambda}}$ for the weighted energy functional $\mathscr{E}_1(t;\lambda)$ in the case $S = 0.1$ using the diffusion-free equilibrium

dissipation is a more (less) efficient process than charge diffusion, and the velocity disturbances would decay more (less) rapidly. For the dielectric liquids used in experiments $10^3 \lesssim M^2/S \lesssim 10^6$, and the former case therefore appears more physically relevant.

4.2. *Conditional stability bounds*

We consider the case of an arbitrary linking parameter λ. Then we have (cf. (3.11) and (4.1))

$$\bar{\bar{\tau}}_\ell^{-1} = \min_{\lambda} \max_{H^*} \left\{ \frac{\langle qE\cdot u + (1-\lambda)\, Qe\cdot u - \lambda(qE\cdot e + Q|e|^2)\rangle}{\langle |\nabla u|^2 + \lambda S q^2\rangle} \right\}, \tag{4.17}$$

and it is readily seen that in this context (cf. (3.12)) A is again given by (4.16). The associated Euler–Lagrange equations for the maximum problem (4.17), on Fourier-decomposing, are equivalent to the linear eigenvalue problem

$$\frac{2}{\tau_\ell}(\mathrm{D}^2-\alpha^2)^2 W + \alpha^2 E(\mathrm{D}^2-\alpha^2)\Phi + \alpha^2(\lambda-1)(\mathrm{D}^2 E)\Phi = 0, \tag{4.18}$$

$$\frac{2\lambda S}{\tau_\ell}(\mathrm{D}^2-\alpha^2)^2\Phi - \lambda[(\mathrm{D}E)\mathrm{D}^2 + (\mathrm{D}^2E)\mathrm{D} - 3\alpha^2 \mathrm{D}E]\Phi + (\mathrm{D}^2-\alpha^2)(EW) + (\lambda-1)(\mathrm{D}^2E)W = 0, \tag{4.19}$$

subject to the eight boundary conditions (4.11). Values of $\bar{\bar{\lambda}}$, α_{crit} and $\bar{\bar{\tau}}_\ell$ obtained from these equations using only the diffusion-free equilibrium are presented in table 2. From (2.14) and (2.15) we find in the limit $C \to 0$ that $E \sim 1$, $\mathrm{D}E \sim C$ and $\mathrm{D}^2E \sim -C^2$, and a leading-order analysis of (4.18) and (4.19) implies

where $$\bar{\bar{\tau}}_\ell \sim \tau_0 C^{-1}, \quad \bar{\bar{\lambda}} \sim \lambda_0 C^{-2}, \quad \Phi \sim \Phi_0 C, \quad W \sim W_0,$$

$$\frac{2}{\tau_0}(\mathrm{D}^2-\alpha^2)^2 W_0 + \alpha^2[\mathrm{D}^2-\alpha^2-\lambda_0]\Phi_0 = 0, \tag{4.20}$$

$$\frac{2\lambda_0}{\tau_0} S(\mathrm{D}^2-\alpha^2)^2\Phi_0 - \lambda_0(\mathrm{D}^2-3\alpha^2)\Phi_0 + (\mathrm{D}^2-\alpha^2-\lambda_0)W_0 = 0. \tag{4.21}$$

Numerical computation then suggests

$$\bar{\bar{\tau}}_\ell C = \tau_0 \approx 80.154, \quad \bar{\bar{\lambda}} C^2 = \lambda_0 \approx 27.8, \quad \alpha_{\text{crit}} \approx 3.95. \tag{4.22}$$

Notice that this analysis is distinct from that given by Atten & Moreau (1972), who,

considering linear instability, found in the limit $C \to 0$ that $TC^2 \approx 220.76214$ (cf. figure 2).

The determination of the attracting radius of conditional stability requires an evaluation of G (cf. (3.14). However, the cubic terms appearing on the right-hand side of (4.1) can be bounded in two different ways. We confine our attention to *two-dimensional* disturbances belonging to $\boldsymbol{H}^*$ which are $2\pi/\alpha$-periodic in x and make use of the embedding inequalities (cf. Joseph 1976). Then first we have

$$-\langle(\lambda-1)\,q\boldsymbol{e}\cdot\boldsymbol{u}+\lambda q|\boldsymbol{e}|^2\rangle \leqslant G\mathscr{E}_1^{\frac{1}{2}}\mathbb{D}, \tag{4.23}$$

where

$$G=\frac{\hat{k}}{(2\lambda S)^{\frac{1}{2}}}\left\{|\lambda-1|+\frac{2}{M\lambda S^{\frac{1}{2}}}[|\lambda-1|+2\lambda]\right\}, \quad \hat{k}^2=\tfrac{1}{2}+\frac{\alpha}{2\pi(1+\alpha^2)^{\frac{1}{2}}}, \tag{4.24}$$

which implies that the bound on $\mathscr{E}_1(0;\lambda)\to\infty$ as $T\to 0$ independently of λ. Secondly, on using the constraint (2.17), we can neglect the term $\lambda Q|\boldsymbol{e}|^2$ in the numerator of (4.17), but we obtain a value $\tau_\ell' \leqslant \tau_\ell$. By a similar analysis we can also find that

$$-\langle|\lambda-1|\,q\boldsymbol{e}\cdot\boldsymbol{u}\rangle \leqslant G'\mathscr{E}_1^{\frac{1}{2}}\mathbb{D}, \tag{4.25}$$

where

$$G'=\frac{\hat{k}|\lambda-1|}{(2\lambda S)^{\frac{1}{2}}}\left[1+\frac{2}{M\lambda S^{\frac{1}{2}}}\right]. \tag{4.26}$$

Here, however, as $\lambda\to 1$ we note that $G'\to 0$, so the bound on $\mathscr{E}_1(0;\lambda)\to\infty$ and $\tau_\ell'\to\tau_1$, the global monotonic bound discussed in §4.1.

For different linking parameters, and therefore for associated functionals, we can now obtain two distinct families of conditional stability curves in the $(T, \mathscr{E}_1(0;\lambda))$-plane. By superimposing these curves we can in principle determine an envelope for $|\boldsymbol{u}(0)|^2+\lambda M^2|\boldsymbol{e}(0)|^2$ as a function of T below which we can guarantee stability in the mean of the equilibrium state (cf. Joseph 1976, fig. (2.1); Deo 1983).

5. The kinetic-charge functional

The evolution equation for the charge functional defined by (2.22) is

$$\frac{\mathrm{d}\mathscr{E}_2}{\mathrm{d}t}=T\langle q\boldsymbol{E}\cdot\boldsymbol{u}+(Q+q)\,\boldsymbol{u}\cdot\boldsymbol{e}-\lambda q\boldsymbol{u}\cdot\boldsymbol{\nabla}Q-\lambda q\boldsymbol{\nabla}\cdot(q\boldsymbol{E}+Q\boldsymbol{e}+q\boldsymbol{e})\rangle$$

$$+\lambda S\langle q\boldsymbol{\nabla}q\rangle_{\mathscr{S}}-\langle|\boldsymbol{\nabla u}|^2+\lambda S|\boldsymbol{\nabla}q|^2\rangle. \tag{5.1}$$

Once again $\mathcal{J}$ is cubic and both $\mathbb{S}$ and $\mathbb{D}$ are quadratic in the perturbations (cf. (3.1)). Unlike the weighted energy functional in the special case $\lambda = 1$, we are unable to bound the cubic terms on the right-hand side of (5.1) by quadratic terms and so obtain a global monotonic stability bound. A variational analysis of the problem specified by (3.2), (3.3) and (5.1) leads to a surface-integral constraint similar to (4.6), but in this case indicates that we must impose ten boundary conditions, which we choose to comprise fluid no-slip, fixed potential, fixed field and fixed charge density at $z = 0$ and $z = 1$. We accordingly define $\boldsymbol{H}^{**}$ as the space of functions

$$\boldsymbol{H}^{**}=\boldsymbol{H}^*(\phi,\boldsymbol{u})\cap\{\phi:\nabla^2\phi|_{z=0}=\nabla^2\phi|_{z=1}=0\}. \tag{5.2}$$

The fact that the surface values of the perturbations $\boldsymbol{e}$ and q must indeed both vanish is related to the postulated existence of monotonic non-autonomous injection and ejection laws that relate the space-charge density to the electrical field at both the emitting and collecting electrodes (cf. Atten & Moreau 1972). Hence we again have the surface functional $\mathbb{S}\equiv 0$.

C	$\bar{\bar{\lambda}}$	α_{crit}	$\bar{\bar{\tau}}_\ell$
0	—	5.731	—
0.001	1.00×10^6	5.731	1.37343×10^5
0.01	1.01×10^4	5.731	1.37963×10^2
0.1	111	5.734	1442.7
1	2.496	5.900	218.809
10	0.87	6.314	133.822
100	0.84	6.33	132.10
1000	0.837	6.330	132.08
∞	0.837	6.330	132.08

TABLE 3. Numerical values of the conditional stability bound $\bar{\bar{\tau}}_\ell$ with corresponding critical wavenumber α_{crit} and optimal linking parameter $\bar{\bar{\lambda}}$ for the kinetic-charge functional $\mathscr{E}_2(t;\lambda)$ in the case $S = 0.1$ using the diffusion-free equilibrium

From (3.11) and (5.1) we have

$$\bar{\bar{\tau}}_\ell^{-1} = \min_{\lambda}\max_{H^{**}} \frac{\langle q\boldsymbol{E}\cdot\boldsymbol{u} + Q\boldsymbol{u}\cdot\boldsymbol{e} - \lambda q\boldsymbol{u}\cdot\boldsymbol{\nabla}Q - \lambda q\boldsymbol{\nabla}\cdot(q\boldsymbol{E}+Q\boldsymbol{e})\rangle}{\langle|\boldsymbol{\nabla u}|^2 + \lambda S|\boldsymbol{\nabla}q|^2\rangle}, \tag{5.3}$$

and the corresponding linear eigenvalue problem after Fourier-decomposing is then

$$\frac{2}{\tau_\ell}(\mathrm{D}^2-\alpha^2)^2\, W + \alpha^2\{[E-\lambda(\mathrm{D}^2E)]\,(\mathrm{D}^2-\alpha^2) - (\mathrm{D}^2E)\}\,\Phi = 0, \tag{5.4}$$

$$\begin{aligned}\frac{2\lambda S}{\tau_\ell}(\mathrm{D}^2-\alpha^2)^3\,\Phi &- \lambda\{3(\mathrm{D}E)\,\mathrm{D}^4 + 6(\mathrm{D}^2E)\,\mathrm{D}^3 + 2[2(\mathrm{D}^3E) - 3\alpha^2(\mathrm{D}E)]\,\mathrm{D}^2 \\ &+ [(\mathrm{D}^4E) - 6\alpha^2(\mathrm{D}^2E)]\,\mathrm{D} + 3\alpha^4(\mathrm{D}E) - 2\alpha^2(\mathrm{D}^3E)\}\,\Phi \\ &- \{[E-\lambda(\mathrm{D}^2E)]\,\mathrm{D}^2 + 2[(\mathrm{D}E) - \lambda^2(\mathrm{D}^3E)]\,\mathrm{D} - \alpha^2E + \lambda\alpha^2(\mathrm{D}^2E) - \lambda(\mathrm{D}^4E)\}\,W = 0,\end{aligned} \tag{5.5}$$

subject to the boundary conditions

$$W = \mathrm{D}W = \Phi = \mathrm{D}\Phi = \mathrm{D}^2\Phi = 0 \quad (z = 0, 1). \tag{5.6}$$

Values of $\bar{\bar{\lambda}}$, α_{crit} and $\bar{\bar{\tau}}_\ell$ obtained by numerical integration of these equations are presented in table 3. Here again we have only used the diffusion-free equilibrium so that $\bar{\tau}_\ell = \tau_\ell$. Furthermore, a leading-order analysis of these latter equations, in the limit $C\to0$, in which

$$\bar{\bar{\tau}}_\ell \sim \tau_0 C^{-1}, \quad \bar{\bar{\lambda}} \sim \lambda_0 C^{-2}, \quad \Phi \sim \Phi_0 C \quad \text{and} \quad W \sim W_0$$

gives

$$\frac{2}{\tau_0}(\mathrm{D}^2-\alpha^2)^2\, W_0 + \alpha^2(1+\lambda_0)\,(\mathrm{D}^2-\alpha^2)\,\Phi_0 = 0, \tag{5.7}$$

$$\frac{2\lambda_0 S}{\tau_0}(\mathrm{D}^2-\alpha^2)^3\,\Phi_0 - 3\lambda_0(\mathrm{D}^2-\alpha^2)^2\,\Phi_0 - (1+\lambda_0)\,(\mathrm{D}^2-\alpha^2)\,W_0 = 0, \tag{5.8}$$

and numerical computation suggests

$$\bar{\bar{\tau}}_\ell C = \tau_0 \approx 137.274, \quad \bar{\bar{\lambda}}C^2 = \lambda_0 \approx 1.0050, \quad \alpha_{\text{crit}} \approx 5.731. \tag{5.9}$$

Similarly the decay rate Λ defined by

$$\Lambda^{-1} = \max_{H^{**}}\left\{\frac{\langle|\boldsymbol{u}|^2 + \bar{\bar{\lambda}}M^2q^2\rangle}{2\langle|\boldsymbol{\nabla u}|^2 + \bar{\bar{\lambda}}S|\boldsymbol{\nabla}q|^2\rangle}\right\} \tag{5.10}$$

is obtained from the decomposed Euler–Lagrange equations

$$\left(\mathrm{D}^2-\alpha^2+\frac{\Lambda M^2}{2S}\right)(\mathrm{D}^2-\alpha^2)^2\,\Phi=0,\quad (\mathrm{D}^2-\alpha^2+\tfrac{1}{2}\Lambda)\,(\mathrm{D}^2-\alpha^2)\,W=0, \tag{5.11}$$

subject to the boundary conditions (5.6). By a similar argument to that leading to (4.16) we find that

$$\Lambda\approx 74.162\min\left(2.01734\frac{S}{M^2},1\right)\quad \alpha_{\mathrm{crit}}\approx(4.530,\,2.399). \tag{5.12}$$

As before we can obtain in two ways bounds on the initial amplitude $\mathscr{E}_2(0;\lambda)$ that guarantee conditional stability. Neither of these, however, approximates to a global monotonic asymptote in the $(T,\mathscr{E}_2(0;\lambda))$-plane, and therefore we do not present them here.

6. The mixed functional

Finally we consider the functional $\mathscr{E}_3(t;\lambda)$ defined by (2.23) and for which the evolution equation is

$$\begin{aligned}\frac{\mathrm{d}\mathscr{E}_3}{\mathrm{d}t}=\;&T\langle qE\cdot(u-e)-(Q+q)\,|e|^2-\lambda q\nabla\cdot(qE+Qe)-\tfrac{1}{2}\lambda q^3-\lambda qu\cdot\nabla Q\rangle\\&+S\langle qe+\lambda q\nabla q-\tfrac{1}{2}\lambda q^2 e\rangle_{\mathscr{S}}-\langle|\nabla u|^2+Sq^2+\lambda S|\nabla q|^2\rangle.\end{aligned} \tag{6.1}$$

As can be seen from (6.1), both the functionals $\mathbb{J}$ and $\mathbb{S}$ are cubic in the perturbations, whilst the dissipation functional $\mathbb{D}$ again is quadratic.

6.1. *Global monotonic bounds*

Since the inequality (2.17) implies that the cubic terms

$$\langle-(Q+q)\,|e|^2-\tfrac{1}{2}\lambda q^3\rangle\leqslant\langle\tfrac{1}{2}\lambda Qq^2\rangle,$$

we can bound $\mathbb{J}$ by a quadratic functional. Furthermore, a variational analysis indicates that the appropriate space of functions over which to maximize is once again $\boldsymbol{H}^{**}$ as defined by (5.2). The vanishing of the space-charge perturbation q on the boundaries then implies that the surface functional $\mathbb{S}$ once again vanishes. Accordingly we obtain an optimal lower bound $\bar{\bar{\tau}}_1$ to a global monotonic bound given by

$$\bar{\bar{\tau}}_1^{-1}=\min_{\lambda}\max_{\boldsymbol{H}^{**}}\left\{\frac{\langle qE\cdot(u-e)-\lambda q\nabla\cdot(qE+Qe)-\lambda qu\cdot\nabla Q+\tfrac{1}{2}\lambda Qq^2\rangle}{\langle|\nabla u|^2+Sq^2+\lambda S|\nabla q|^2\rangle}\right\}, \tag{6.2}$$

and corresponding Λ given by

$$\Lambda^{-1}=\max_{\boldsymbol{H}^{**}}\left\{\frac{\langle|u|^2+M^2|e|^2+\bar{\bar{\lambda}}M^2q^2\rangle}{2\langle|\nabla u|^2+Sq^2+\bar{\bar{\lambda}}S|\nabla q|^2\rangle}\right\}. \tag{6.3}$$

The Euler–Lagrange equations associated with the maximum problem (6.2) are

$$\frac{2}{\tau_1}\nabla^2(\nabla\wedge u)+\nabla q\wedge E+\lambda\nabla Q\wedge\nabla q=0, \tag{6.4}$$

$$\begin{aligned}\frac{2S}{\tau_1}(\lambda\nabla^2-1)\,\nabla^2 q+\lambda\nabla^2[E\cdot\nabla q-u\cdot\nabla Q+Qq-\nabla\cdot(Qe+qE)]\\+\nabla^2[E\cdot(u-e)]-\nabla\cdot(\lambda Q\nabla q-qE)=0,\end{aligned} \tag{6.5}$$

C	$\bar{\bar{\lambda}}$	α_{crit}	$\bar{\bar{\tau}}_1$	$\bar{\bar{\tau}}_2(\bar{\bar{\lambda}})$
(0)	—	(5.748)	—	—
0.001	(1.006×10^6)	(5.748)	(9.650×10^4)	(1.497×10^5) [$a=6.0$]
0.01	(1.015×10^4)	(5.748)	(9.693×10^3)	(1.504×10^4) [$a=6.0$]
0.1	111	5.751	1015.4	1.573×10^3
	(110)	(5.750)	(1013.6)	(1.573×10^3) [$a=6.0$]
1	2.513	5.859	153.0	240.7
	(2.515)	(5.860)	(152.98)	(240.6) [$a=6.0$]
10	0.825	6.216	89.47	150.4
	(0.87)	(6.195)	(91.74)	(152.3) [$a=6.5$]
100	0.595	6.256	80.01	144
	(0.84)	(6.2)	(90.3)	(151) [$a=6.5$]
500	0.357	6.6	67	128.3 [$a=6.5$]
1000	(0.84)	(6.2)	(90.3)	(151) [$a=6.5$]
(∞)	(0.84)	(6.2)	(90.3)	(151) [$a=6.5$]

TABLE 4. Numerical values of the global monotonic stability bound $\bar{\bar{\tau}}_1$ with corresponding critical wavenumber α_{crit} and optimal linking parameter $\bar{\bar{\lambda}}$ together with trial-function estimates $\bar{\bar{\tau}}_2$ at specified wavenumber a for the mixed functional $\mathscr{E}_3(t;\lambda)$ in the case $S=0.1$. Results in parenthesis are those obtained for the diffusion-free equilibrium.

together with (2.16*d–f*). Normal-mode analysis then gives

$$\frac{2}{\tau_1}[\mathrm{D}^2-\alpha^2]^2\,W+\alpha^2[E-\lambda(\mathrm{D}^2E)]\,(\mathrm{D}^2-\alpha^2)\,\Phi=0, \tag{6.6}$$

$$\begin{aligned}\frac{2S}{\tau_1}[\mathrm{D}^2-\alpha^2]^2[\lambda(\mathrm{D}^2-\alpha^2)-1]\,\Phi-\{&2\lambda(\mathrm{D}E)\,\mathrm{D}^4+4\lambda(\mathrm{D}^2E)\,\mathrm{D}^3+[3\lambda(\mathrm{D}^3E)\\&-4\lambda\alpha^2(\mathrm{D}E)+(\mathrm{D}E)]\,\mathrm{D}^2+[\lambda(\mathrm{D}^4E)-4\lambda\alpha^2(\mathrm{D}^2E)+(\mathrm{D}^2E)]\,\mathrm{D}\\&-\lambda\alpha^2(\mathrm{D}^3E)+2\lambda\alpha^4(\mathrm{D}E)+\alpha^2(\mathrm{D}E)\}\,\Phi-\{[E-\lambda(\mathrm{D}^2E)]\,\mathrm{D}^2\\&+2[(\mathrm{D}E)-\lambda(\mathrm{D}^3E)]\,\mathrm{D}-\alpha^2E+(\lambda\alpha^2+1)\,(\mathrm{D}^2E)-\lambda(\mathrm{D}^4E)\}\,W=0,\end{aligned} \tag{6.7}$$

subject to the boundary conditions (5.6). The resulting values of $\bar{\bar{\lambda}}$, α_{crit} and $\bar{\bar{\tau}}_1$ obtained numerically for both the diffusion and diffusion-free equilibria are presented in table 4 together with estimates $\bar{\bar{\tau}}_2$ using y-independent trial functions of the form

$$\phi=z^3(1-z)^3\sin ax, \tag{6.8}$$

$$\boldsymbol{u}=[2z(1-z)\,(1-2z)\cos ax,\ 0,\ az^2(1-z)^2\sin ax], \tag{6.9}$$

where a is an x-directional wavenumber. Once again for the diffusion-free equilibrium case, a leading-order analysis as $C\to0$ leads to equations

$$\frac{2}{\tau_0}(\mathrm{D}^2-\alpha^2)^2\,W_0+\alpha^2(1+\lambda_0)\,(\mathrm{D}^2-\alpha^2)\,\Phi_0=0, \tag{6.10}$$

$$\frac{2S\lambda_0}{\tau_0}(\mathrm{D}^2-\alpha^2)^3\,\Phi_0-2\lambda_0(\mathrm{D}^2-\alpha^2)^2\,\Phi_0-(1+\lambda_0)\,(\mathrm{D}^2-\alpha^2)\,W_0=0, \tag{6.11}$$

so that

$$\bar{\bar{\tau}}_1C=\tau_0\approx96.517;\quad \bar{\bar{\lambda}}C^2=\lambda_0\approx1.003,\quad \alpha_{\text{crit}}\approx5.748. \tag{6.12}$$

λ	$N(\lambda)$	$A(\lambda)$
∞ $(C=0)$	2.017	4.530
1.00096×10^{6} $(C\approx10^{-3})$	2.017	4.530
1.0147×10^{4} $(C\approx10^{-2})$	2.017	4.530
110.9 $(C\approx10^{-1})$	2.017	4.530
2.5147 $(C\approx1)$	2.012	4.510
0.87 $(C\approx10)$	2.002	4.467
0.83 $(C>10^{2})$	2.001	4.464

TABLE 5. Values of decay-rate parameter $N(\lambda)$ and associated wavenumber parameter $A(\lambda)$

The maximum problem defined by (6.3) now leads to Euler–Lagrange equations

$$(\bar{\bar{\lambda}}\nabla^2-1)\left[\frac{2S}{\Lambda M^2}\nabla^2+1\right]\nabla^2\Phi=0,\quad \frac{2}{\Lambda}\nabla^2(\boldsymbol{\nabla}\wedge\boldsymbol{u})+\boldsymbol{\nabla}\wedge\boldsymbol{u}=0,\quad \boldsymbol{\nabla}\cdot\boldsymbol{u}=0, \tag{6.13}$$

which in normal-mode form become

$$[\bar{\bar{\lambda}}(\mathrm{D}^2-\alpha^2)-1]\left[\frac{2S}{\Lambda M^2}(\mathrm{D}^2-\alpha^2)+1\right][\mathrm{D}^2-\alpha^2]\Phi=0,$$

$$(\mathrm{D}^2-\alpha^2+\tfrac{1}{2}\Lambda)(\mathrm{D}^2-\alpha^2)W=0, \tag{6.14}$$

subject to the boundary conditions (5.6). Here, however, Λ depends upon $\bar{\bar{\lambda}}$, which of course depends upon the injection parameter C. We may write then

$$\Lambda\approx74.162\min\left[N(\bar{\bar{\lambda}})\frac{S}{M^2},1\right],\quad \alpha_{\mathrm{crit}}\approx[A(\bar{\bar{\lambda}}),2.399], \tag{6.15}$$

where $N(\lambda)$ and $A(\lambda)$ are slowly varying functions and given for selected values of λ in table 5. We note that with the diffusion-free equilibrium in the limit $C\to0$ for which $\bar{\bar{\lambda}}\to\infty$ this problem is identical with that of (5.11) with solution (5.12) so that $N(\bar{\bar{\lambda}})\to2.017$ and $A(\bar{\bar{\lambda}})\to4.530$.

6.2. *Conditional stability bounds*

From (3.11) and (6.1) we have

$$\bar{\bar{\tau}}_\ell^{-1}=\min_{\lambda}\max_{H^{**}}\left\{\frac{\langle q\boldsymbol{E}\cdot(\boldsymbol{u}-\boldsymbol{e})-Q|\boldsymbol{e}|^2-\lambda q\boldsymbol{\nabla}\cdot(q\boldsymbol{E}+Q\boldsymbol{e})-\lambda q\boldsymbol{u}\cdot\boldsymbol{\nabla}Q\rangle}{\langle|\boldsymbol{\nabla}\boldsymbol{u}|^2+Sq^2+\lambda S|\boldsymbol{\nabla}q|^2\rangle}\right\}, \tag{6.16}$$

with corresponding Euler–Lagrange equations in normal-mode form

$$\frac{2}{\tau_\ell}[\mathrm{D}^2-\alpha^2]^2W+\alpha^2[E-\lambda(\mathrm{D}^2E)](\mathrm{D}^2-\alpha^2)\Phi=0, \tag{6.17}$$

$$\begin{aligned}\frac{2S}{\tau_\ell}[\mathrm{D}^2-\alpha^2]^2[\lambda(\mathrm{D}^2-\alpha^2)-1]\Phi&-\{3\lambda(\mathrm{D}E)\,\mathrm{D}^4+6\lambda(\mathrm{D}^2E)\,\mathrm{D}^3\\&+[4\lambda(\mathrm{D}^3E)-6\lambda\alpha^2(\mathrm{D}E)+(\mathrm{D}E)]\,\mathrm{D}^2+[\lambda(\mathrm{D}^4E)-6\lambda\alpha^2(\mathrm{D}^2E)\\&+(\mathrm{D}^2E)]\,\mathrm{D}-2\lambda\alpha^2(\mathrm{D}^3E)+3\lambda\alpha^4(\mathrm{D}E)-3\alpha^2(\mathrm{D}E)\}\Phi\\&-\{[E-\lambda(\mathrm{D}^2E)]\,\mathrm{D}^2+2[(\mathrm{D}E)-\lambda(\mathrm{D}^3E)]\,\mathrm{D}-\alpha^2E\\&+(\lambda\alpha^2+1)(\mathrm{D}^2E)-\lambda(\mathrm{D}^4E)\}W=0,\end{aligned} \tag{6.18}$$

C	$\bar{\bar{\lambda}}$	α_{crit}	$\bar{\bar{\tau}}_\ell$
0	—	5.731	—
0.001	1.00×10^6	5.73	1.3734×10^5
0.01	1.01×10^4	5.73	1.379×10^4
0.1	110.4	5.73	1.4426×10^3
1	2.49	5.88	218.20
10	0.86	6.27	132.78
100	0.831	6.28	131.08
1000	0.83	6.28	131.1
∞	0.83	6.29	131.1

TABLE 6. Numerical values of the conditional stability bound $\bar{\bar{\tau}}_\ell$ with corresponding critical wavenumber α_{crit} and optimal linking parameter $\bar{\bar{\lambda}}$ for the mixed functional $\mathscr{E}_3(t;\lambda)$ in the case $S = 0.1$ using the diffusion-free equilibrium

subject to the boundary conditions (5.6). The corresponding values of $\bar{\bar{\lambda}}$, α_{crit} and $\bar{\bar{\tau}}_\ell$ obtained numerically for the diffusion-free equilibrium are presented in table 6. In the limit $C \to 0$, since $\bar{\bar{\lambda}} \sim \lambda_0 C^{-2}$, $\Phi \sim \Phi_0 C$ and $W \sim W_0$, the functional $\mathscr{E}_3(t;\bar{\bar{\lambda}};\phi,\boldsymbol{u}) \sim \mathscr{E}_2(t;\lambda_0;\phi_0,\boldsymbol{u}_0)$. Hence the solution of the problem (6.17), (6.18) and (5.6) in this limit is given by (5.9). The corresponding problem for the determination of Λ as defined by (6.3) is specified by (6.14) and (5.6) with solution given by (6.15). In this case also we can obtain attracting radii for the initial amplitude $\mathscr{E}_3(0;\lambda)$ that guarantee conditional stability though we do not present them here.

7. Numerical analysis

All numerical calculations were carried out on Honeywell Multics/ICL 2980 machines using a Chebyshev collocation technique in which the unknown functions were represented by a finite series of Chebyshev polynomials. The diffusion equilibria were evaluated and the resulting linear algebraic systems were solved using standard library routines. The degree of approximation required to give the accuracy to which the results are quoted was usually 30 although checks were made using polynomials of degree up to and including 35.

Owing to the singular perturbation nature of the diffusion equilibrium (2.12) and (2.13), numerical difficulties were encountered for injection strengths $C < 0.1$ and $C > 500$ when using the functional $\mathscr{E}_3(t;\lambda)$. The solution $\bar{\tau}$ of $\tau(\lambda,\bar{\tau}) = \bar{\tau}$ was found by an iteration scheme operating on values of τ minimized over wavenumber α, and estimates $\bar{\bar{\tau}}$ were then found by maximizing over the linking parameter λ using quadratic curve-fitting routines. In order to guarantee good convergence of the Chebyshev series and to avoid the problem of ill-conditioning it was found necessary to filter the equations before processing. For (4.18) and (4.19) subject to the boundary conditions (4.11), greater accuracy was achieved for $C \lesssim 0.1$ by solving for $C\tau$, $C^2\lambda$, $C^{-1}\Phi(z)$ and $W(z)$. On the other hand, for (5.4), (5.5), (6.6), (6.7) and (6.17), (6.18) subject to the boundary conditions (5.6), greater accuracy was achieved for $C \gtrsim 10$ by solving for $z\Phi(z)$ and $zW(z)$ with appropriately modified boundary conditions.

The trial functions for the energy functional $\mathscr{E}_1(t;1)$ for ϕ and $\boldsymbol{u}$ given by (4.12) and (4.13) were chosen to have a single-cell z-dependence satisfying boundary constraints (4.11) and sinusoidal x-dependence with a specified wavenumber a. The fact that the cubic production integrals then vanished meant that the ratio of

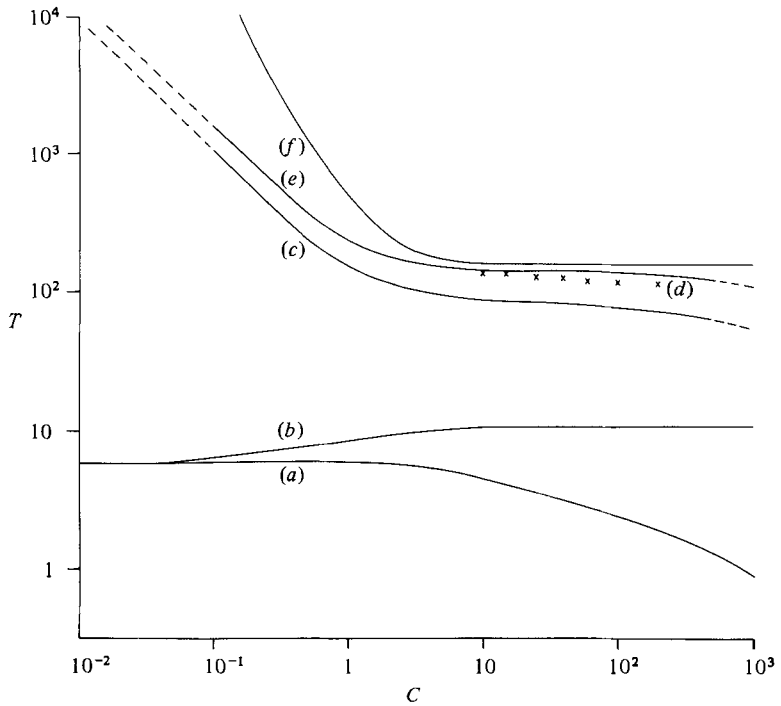

FIGURE 1. Variations of the optimized stability criteria with injection parameter C for the diffusion equilibrium ($S = 0.1$): (*a*) global monotonic $\bar{\tau}_1$ values for $\mathscr{E}_1(t;1)$; (*b*) global monotonic $\bar{\tau}_2$ values for $\mathscr{E}_1(t;1)$; (*c*) global monotonic $\bar{\bar{\tau}}_1$ values for $\mathscr{E}_3(t;\lambda)$; (*d*) linear instability results for fixed $S/T = 5 \times 10^{-3}$ after Atten (1976); (*e*) global monotonic $\bar{\bar{\tau}}_2$ values for $\mathscr{E}_3(t;\lambda)$; (*f*) linear diffusion-free instability curve of Atten & Moreau (1972).

production to dissipation integrals became homogeneous of degree two in the amplitudes of ϕ and $\boldsymbol{u}$. The ratio of these amplitudes was then determined analytically so as to minimize $\bar{\tau}_2$. The trial functions for the mixed functional $\mathscr{E}_3(t;\lambda)$ given by (6.8) and (6.9) satisfying boundary constraints (5.6) were similarly chosen. However, in this case an algebraic z-dependence proved to give a lower value of $\bar{\bar{\tau}}_2$ than that provided by a trigonometrical z-dependence.

8. Discussion and concluding remarks

All the foregoing eigenvalue problems involving the parameter S were solved numerically in the case $S = 0.1$. This value was chosen as being representative of typical experimental dielectric liquids. The resulting stability criteria as functions of the injection strength parameter C are given in tables 1–4 and 6 and illustrated in figures 1 and 2.

The global monotonic lower bound $\bar{\tau}_1$ of $\bar{\tau}$ resulting from using the energy functional $\mathscr{E}_1(t;1)$ is clearly seen (cf. table 1) to be relatively insensitive to injection-strength values $C \lesssim 1$. For larger values of C we see a marked destabilizing influence of charge diffusion, and the one-dimensional nature of the most-energetic disturbance ($\alpha_{\text{crit}} = 0$). On the other hand, the global monotonic lower bound resulting from using the energy functional $\mathscr{E}_1(t;1)$ with the diffusion-free equilibrium is clearly seen to be relatively insensitive to the value of injection strength. In the case of weak injection ($C \ll 1$) we obtain within the context of this model, with potential and electrical field

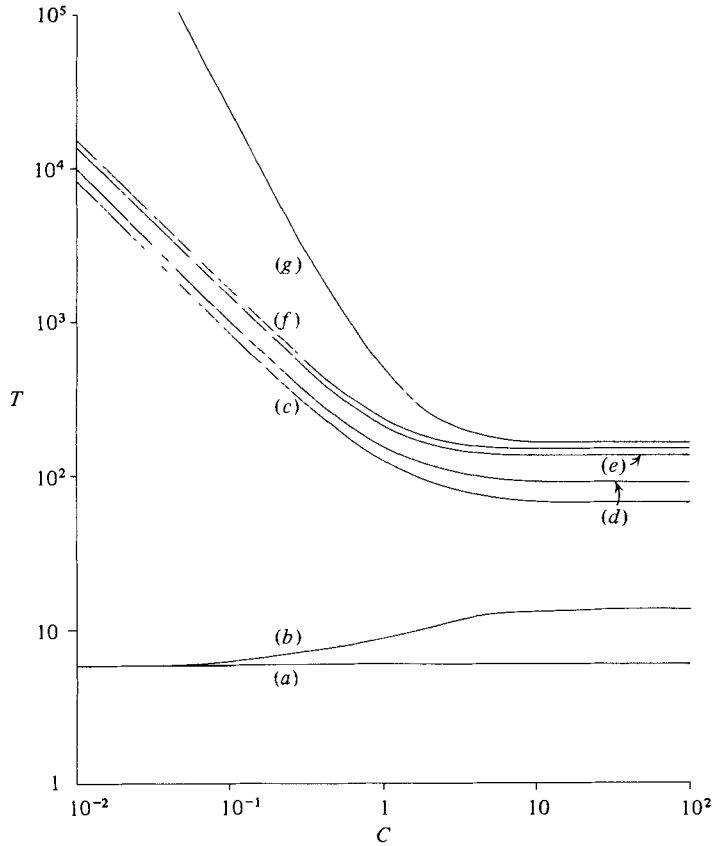

FIGURE 2. Variations of the optimized stability criteria with injection parameter C for the diffusion-free equilibrium ($S = 0.1$): (*a*) global monotonic τ_1 values for $\mathscr{E}_1(t;1)$; (*b*) global monotonic τ_2 values for $\mathscr{E}_1(t;1)$; (*c*) conditional monotonic $\bar{\bar{\tau}}_\ell$ values for $\mathscr{E}_1(t;\lambda)$; (*d*) global monotonic $\bar{\bar{\tau}}_1$ values for $\mathscr{E}_3(t;\lambda)$; (*e*) conditional monotonic $\bar{\bar{\tau}}_\ell$ values for $\mathscr{E}_2(t;\lambda)$; [$\simeq$ conditional monotonic $\bar{\bar{\tau}}_\ell$ values for $\mathscr{E}_3(t;\lambda)$]; (*f*) global monotonic $\bar{\bar{\tau}}_2$ values for $\mathscr{E}_3(t;\lambda)$; (*g*) linear instability curve of Atten & Moreau (1972).

fixed on the electrodes, finite values of $\bar{\bar{\tau}}_1$ and the upper global monotonic bounds $\bar{\bar{\tau}}_2$. In any case of strong injection ($C \gg 1$) all four bounds are well below any previously determined experimental and theoretical values.

The global monotonic lower and upper bounds $\bar{\bar{\tau}}_1$ and $\bar{\bar{\tau}}_2(\bar{\bar{\lambda}})$ of $\bar{\bar{\tau}}$ resulting from using the mixed functional $\mathscr{E}_3(t;\lambda)$ (cf. table 4), incorporating electrical boundary conditions $\Phi = \mathrm{D}\Phi = \mathrm{D}^2\Phi = 0$ at $z = 0$ and 1, demonstrate in the limit $C \to 0$ the asymptotic behaviour $TC \approx 96.5$ and $TC \approx 150$. Whilst for large C space-charge-diffusion effects demonstrate a destabilizing influence, in the $C \to \infty$ limit the diffusion-free equilibrium suggests an asymptotic behaviour $T \approx 90.3$, and $T \approx 151$ respectively. As might have been expected, imposing the extra constraint of fixed charge on the electrodes tends to stabilize the system. A further comparison may be made with the bound of the diffusion-free linear instability analysis of Atten & Moreau (1972), incorporating, for finite C, $\Phi = \mathrm{D}^2\Phi = 0$ at $z = 0$ and $\Phi = 0$ at $z = 1$, for which, in the limit $C \to 0$, $TC^2 \approx 221$, and incorporating, for infinite C, $\Phi = \mathrm{D}\Phi = 0$ at $z = 0$ and $\Phi = 0$ at $z = 1$ for which $T \approx 161$. Atten's (1976) instability results of a diffusion equilibrium unfortunately are not readily comparable with the above, since for a fixed injection

Liquid and injection ions	Relative permittivity ϵ/ϵ_0	M	S	T_{exp}	$\bar{\bar{\tau}}_1$	$(\bar{\bar{\tau}}_1)$
Chlorobenzene Cl^-	6	4.9	0.037	88	76	(85)
Pyralene 1460 Cl^-	5.9	60	0.041	82	75	(85)
Model liquid	—	—	0.1	—	67	(90.3)
Nitrobenzene Cl^-	35	22	0.21	92	62	(98)
Propylene carbonate Cl^-	69	51	0.44	88	60	(110)

TABLE 7. Values of the optimized global monotonic bound $\bar{\bar{\tau}}$, obtained from the mixed functional $\mathscr{E}_3(t;\lambda)$. $\bar{\bar{\tau}}_1$ corresponds to $C = 500$ and $(\bar{\bar{\tau}}_1)$ refers to the limit $C \to \infty$ for the diffusion-free equilibrium. Physical data and experimental instability results after Lacroix *et al.* (1975) are included for comparison.

strength and ratio S/T his calculated value of T corresponds to a specific value of S. Hence different values of C provide linear instability limits T relevant to differing dielectric liquids. His results, however, for the case $S/T = 5 \times 10^{-3}$ are included in figure 1.

It is evident from tables 2, 3 and 6 that the conditional stability bounds $\bar{\bar{\tau}}_\ell$ from $\mathscr{E}_1(t;\lambda)$, $\mathscr{E}_2(t;\lambda)$ and $\mathscr{E}_3(t;\lambda)$ exhibit similar asymptotic behaviours to the corresponding diffusion-free global monotonic lower bound $\bar{\bar{\tau}}_1$ of the mixed functional $\mathscr{E}_3(t;\lambda)$. For $\mathscr{E}_1$, $\mathscr{E}_2$ and $\mathscr{E}_3$ we have the asymptotic behaviour $TC \approx 80.15$, 137.3 and 137.3 respectively in the limit $C \to 0$, and $T \approx 66.8$, 132.1 and 131.1 respectively in the $C \to \infty$ limit. Indeed the results from the charge functionals $\mathscr{E}_2(t;\lambda)$ and $\mathscr{E}_3(t;\lambda)$ are very similar, as perhaps might have been expected in that they incorporate identical electrical and fluid-dynamic boundary conditions. Moreover, these values of $\bar{\bar{\tau}}_\ell$ are also upper bounds of $\bar{\bar{\tau}}$, which in the case of the mixed functional provide better upper constraints than those given by the trial-function values $\bar{\bar{\tau}}_2$. It must be remembered, however, that both the conditional stability bounds and trial-function estimates were obtained for two-dimensional disturbances only. However, it can be easily verified that taking trial functions with a hexagonal planform produces results identical with those possessing a two-dimensional roll character.

Certainly using a diffusion-free equilibrium the optimal value $\bar{\bar{\lambda}}$ of the linking parameter λ in each functional (cf. tables 2–4 and 6) exhibits an asymptotic behaviour $\bar{\bar{\lambda}} \to$ constant in the limit $C \to \infty$, but a behaviour $\bar{\bar{\lambda}} C^2 \to$ constant in the limit $C \to 0$. In addition in this latter limit $\Phi = O(C^{-1})$ and $W = O(1)$. Thus this method of analysis ensures that the fluid-dynamic and electrical contributions to each of the functionals considered are scaled so as to be of similar magnitude.

Whilst the functionals implicitly involve the parameter M, the global and conditional stability bounds are independent of it. Even the decay-rate measure Λ is only indirectly affected by M, and is actually only a function of the electrical Prandtl number. This latter non-dimensional number essentially measures the importance of viscous to charge diffusion processes. As already mentioned for typical experimental dielectric liquids $10^3 \lesssim \nu/D_c \lesssim 10^6$, perhaps suggesting that charge diffusion is not, at least in the mainstream, of major importance, though for a successful application of energy stability theory it cannot be neglected totally. By comparing the results using a diffusion-free equilibrium with those obtained by retaining diffusion completely we find that only for large C does charge diffusion manifest its destabilizing influence. For small values of injection strength and for

$S = 0.1$ the resulting bounds on T imply $S/T = D_c/K\Phi_0 \lesssim 2 \times 10^{-2}$, possibly justifying the neglect of diffusion.

Perhaps the most striking result of this analysis has been the monotonic global stability bound of 67 in the case $C = 500$ and 90.3 in the diffusion-free SCLC limit $C \to \infty$ obtained from the mixed functional with $S = 0.1$ and using the physical constraint of total space charge always remaining non-negative. Numerical computations were also carried out for the specific liquids pyralene 1460, chlorobenzene, nitrobenzene and propylene carbonate, and are presented in table 7. It can be seen that the analytically determined diffusion-incorporated bounds $\bar{\bar{\tau}}_1$ on stability are all inferior to the experimental results $T_{\exp}$. It is perhaps worth noting that the value of $\bar{\bar{\tau}}_1$ decreases as S increases, reflecting the destabilizing effect of diffusion, whereas the diffusion-free value increases as S increases, once again stressing the necessity of including diffusion at every stage in the analysis. Nevertheless the assumptions implicitly made in this model, including the boundary constraints, are only approximations to those occurring in the laboratory. A better understanding of the physical context might lead to the construction of more physically relevant functionals.

Appendix

Strictly we require analytic proofs of the existence of finite maxima for τ_1^{-1}, τ_ℓ^{-1} and Λ^{-1} for each of the functionals considered. We present as a typical example that corresponding to τ_ℓ^{-1} for the mixed functional $\mathscr{E}_3(t;\lambda)$ defined by (cf. (6.16))

$$\tau_\ell^{-1} = \max_{H^{**}} \left\{ \frac{\langle qE\cdot(u-e) - Q|e|^2 - \lambda q \nabla\cdot(qE+Qe) - \lambda q u\cdot\nabla Q\rangle}{\langle |\nabla u|^2 + Sq^2 + \lambda S|\nabla q|^2\rangle} \right\}, \tag{A 1}$$

where H^{**} is defined by (3.5), (4.7) and (5.2). Then H^{**} is a space of almost-periodic smooth functions for which $e = -\nabla\phi$ and $q = \nabla\cdot e$, and ϕ, e and q vanish on bounding surfaces. Now

$$\begin{aligned}\langle q^2\rangle &= \langle(\partial_1 e_1)^2 + (\partial_2 e_2)^2 + (\partial_3 e_3)^2 + 2(\partial_1 e_1)(\partial_2 e_2) + 2(\partial_2 e_2)(\partial_3 e_3) + 2(\partial_1 e_1)(\partial_3 e_3)\rangle \\ &= \langle(\partial_1 e_1)^2 + (\partial_2 e_2)^2 + (\partial_3 e_3)^2 + 2(\partial_1 e_2)^2 + 2(\partial_3 e_1)^2 + 2(\partial_3 e_2)^2\rangle, \end{aligned} \tag{A 2}$$

so that

$$\frac{\langle |e|^2\rangle}{\langle q^2\rangle} \leqslant \frac{\langle e_1^2\rangle}{2\langle(\partial_3 e_1)^2\rangle} + \frac{\langle e_2^2\rangle}{2\langle(\partial_3 e_2)^2\rangle} + \frac{\langle e_3^2\rangle}{\langle(\partial_3 e_3)^2\rangle}. \tag{A 3}$$

Joseph (1976, p. 13) has shown that $\langle\theta^2\rangle/\langle|\nabla\theta|^2\rangle$, where θ is a smooth function vanishing on the boundaries, is bounded above. Hence from (A 3) we can assert that $\langle|e|^2\rangle/\langle q^2\rangle$ is also bounded above.

If we confine our attention to cases of finite non-zero injection parameter C and use the equilibrium properties $E(z) \leqslant E(1)$ and $Q(z) \leqslant Q(0)$ for all $z \in [0,1]$, where $E(1)$ and $Q(0)$ are finite quantities, together with integration by parts, we can write

$$\begin{aligned}\tau_\ell^{-1} &\leqslant \frac{\langle(\lambda+1)(|u|^2+|e|^2) + (\lambda+2)E^2(1)q^2 + \lambda[2Q^2(0)+1]|\nabla q|^2\rangle}{2\langle|\nabla u|^2 + Sq^2 + \lambda S|\nabla q|^2\rangle} \\ &\leqslant \frac{(\lambda+1)\langle|u|^2\rangle}{2\langle|\nabla u|^2\rangle} + \frac{(\lambda+1)\langle|e|^2\rangle}{2S\langle q^2\rangle} + \frac{(\lambda+2)E^2(1) + [2Q^2(0)+1]}{2S}. \end{aligned} \tag{A 4}$$

Once again Joseph (1976, p. 13) has shown that $\langle|u|^2\rangle/\langle|\nabla u|^2\rangle$, where u is a smooth solenoidal vector field vanishing on the boundaries, is bounded above. Then from (A 3) and (A 4) we have τ_ℓ^{-1} bounded above, as required.

REFERENCES

ATTEN, P. 1975 Electrohydrodynamic stability of liquids subjected to unipolar injection. In *Proc. Intl Conf. on Conduction and Breakdown in Dielectric Liquids, Delft*, p. 119.

ATTEN, P. 1976 Rôle de la diffusion dans le problème de la stabilité hydrodynamique d'un liquide diélectrique soumis à une injection unipolaire forte. *C.R. Acad. Sci. Paris* **283B**, 29.

ATTEN, P. & LACROIX, J. C. 1974 Stabilité hydrodynamique non-linéaire d'un liquide isolant soumis à une injection unipolaire forte. *C.R. Acad. Sci. Paris* **278B**, 385.

ATTEN, P. & LACROIX, J. C. 1978 Electrohydrodynamic stability of liquids subjected to unipolar injection: nonlinear phenomena. *J. Electrostat.* **5**, 439.

ATTEN, P. & LACROIX, J. C. 1979 Nonlinear hydrodynamic stability of liquids subjected to unipolar injection. *J. Méc.* **18**, 469.

ATTEN, P. & MOREAU, R. 1972 Stabilité électrohydrodynamique des liquides isolants soumis à une injection unipolaire. *J. Méc.* **11**, 471.

DEO, B. J. S. 1983 Generalised energy stability analyses of electrohydrodynamic equilibria. Ph.D. thesis, University of Bristol.

DEO, B. J. S. & RICHARDSON, A. T. 1983 Submitted to *Q. J. Mech. Appl. Maths.*

JOSEPH, D. D. 1976 *Stability of Fluid Motions* I and II. Springer.

LACROIX, J. C., ATTEN, P. & HOPFINGER, E. J. 1975 Electroconvection in a dielectric liquid layer subjected to unipolar injection. *J. Fluid Mech.* **69**, 539.

RICHARDSON, A. T. 1980 The linear instability of a dielectric liquid contained in a cylindrical annulus and subjected to unipolar charge injection. *Q. J. Mech. Appl. Maths* **33**, 277.